LAYERED MANTLE CONVECTION AND MAGMA PRODUCTION ON MARS: EFFECTS OF DENSE LAYER PROPERTIES. Qingsong Li and Walter S. Kiefer, Lunar and Planetary Institute, 3600 Bay Area Blvd., Houston TX 77058 (li@lpi.usra.edu).

Introduction: Geologically recent volcanism on Mars [1-4] can be well explained with mantle convection and plumes [5-7]. Most of these studies have assumed single layer convection in Martian mantle. However, a layered Martian mantle has been suggested in the model of magma ocean and mantle overturn [8]. The possible effects of such stratification on the early volcanism, magnetic dynamo, and thermal history of Mars were explored before [9-11]. We did preliminary exploration of the effect of a deep dense layer on mantle convection and magma production of Mars by fixing the core-mantle boundary temperature [12]. Here, we explore the effects of dense layer properties on mantle convection and magma production by fixing the layer interface temperature. Our focus is on the viscosity and radioactivity contrast between the two layers.

Computational Approach: We use the spherical axi-symmetric version of CitCOM [13, 14] to simulate mantle convection on Mars. A particle ratio method [15] is used in the code to model thermochemical convection. The non-dimensional model domain (θ = 0-π/4, R = 1-2) is meshed with a 128×160 grid that has a typical mesh resolution of 13 km in the upper layer and 4 km in the lower layer. Each element is assigned with 16 particles to trace chemical composition. The upper and lower boundaries are constant in temperature. The side boundaries are thermally insulated. All four boundaries are free-slip. The mantle viscosity is temperature dependent, obeying the Arrhenius viscosity law [16]. The activation energy is 160 kJ/mole [5]. Half of the radioactive elements [17] are differentiated into the crust. The buoyancy number, B, is the ratio between the chemical density difference between the layers and the thermal buoyancy [18]. We assume B=1, corresponding to a density difference of about 200 kg m^{-3} between the two layers. The actual density difference could be larger [8], but further increase in B does not modify the fluid dynamics [18]. The dimensional model parameters are the same as in [5]. An initial thermal perturbation is applied to generate a plume at the center of the model. The model has been run to reach a statistically steady-state for each model case.

We use Katz's melt fraction calculation formula, in which melt fraction is a function of solidus, liquidus and the mantle temperature [19]. The Katz's dry solidus model coincides well with the experimental results of martian analog composition [20]. Magma production is calculated using the formalism of Kiefer [6].

In model parameters input and model results analysis, the core-mantle boundary temperature is set to dimensionalize the temperature fields. In our previous studies [12], we keep the core-mantle boundary temperature fixed among model cases. Since the upper layer behaves similar to a single layer convection when B>1 [21], we choose to fix the layer interface temperature here. This is accomplished through iteration. First, we give a try core-mantle boundary temperature. Second, we obtain a horizontally averaged interface temperature through model simulation. Third, we update the core-mantle boundary temperature to scale the layer interface temperature to be 1600 °C. These steps are iterated for 2-3 times to let the interface temperature be within 1600 °C ± 20°C among model cases.

Results: The thickness of the dense layer is not well constrained and model dependent [22, 23], so we consider a range of bottom layer thickness (40-180 km). We also consider a range of convective vigor (thermal Rayleigh number of the upper layer defined using the volume average viscosity varies from 2.3×10^6 to 1.3×10^7), and viscosity and radioactivity contrast between the upper and lower layers. An example thermal field is shown in Figure 1. Model parameters for this example case are: thickness of the chemical layer is 180 km; the volume-averaged thermal Ra of the upper layer is 6.5×10^6; activation energy is 160 kJ/mole; half of the radioactivity is in the crust; and mantle viscosity and radioactivity are the same between the two layers.

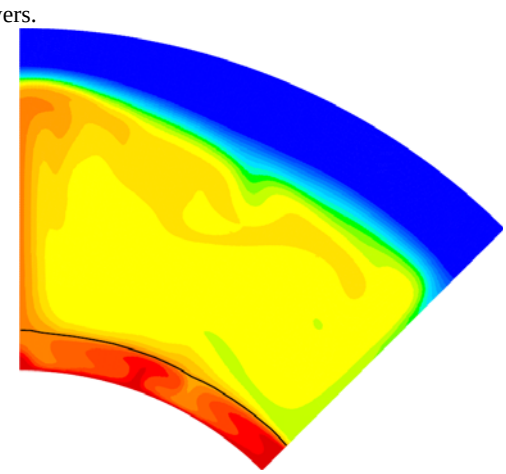

Figure 1. The super-adiabatic non-dimensional temperature is shown for the example case (see text). Color scale is 0.5 – 1.0 (blue to red). Temperature less than 0.5 is shown as blue. The black curve is the upper boundary of the dense layer.

In previous studies [12, 18], the core heat flux is suppressed by the inefficient heat transfer through the dense layer when the core-mantle boundary temperature is fixed. Here, we fix the layer interface temperature instead. Then the core heat flux is a function of the upper layer Rayleigh number (Figure 2), while the existence and thickness of the dense layer has limited effects on heat fluxes. This is con-

sistent with experimental results of B>1 in mobile-lid convection [21].

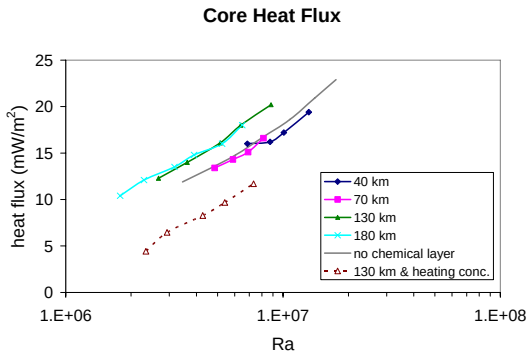

Figure 2. Core heat flux vs upper layer Ra for models with dense layer thickness of 40-180 km. In the case of radioactivity elements concentration in the lower layer, the crustal radioactivity element is kept constant, while the dense layer radioactivity increases and becomes identical to the crustal concentration.

According to our previous study [12] when the core-mantle boundary temperature is fixed, the existence of a dense layer causes both cooler plume and thicker lithosphere, thus makes it harder for decompression melting at the plume head. However, with our new temperature scaling, the existence of dense layer has limited effects on magma production (Figure 3). Although the heat transfer is less efficient in a layered mantle, the core-mantle boundary temperature becomes larger as the layer interface temperature is fixed. Thus, the magma production rate of layered convection is similar to single layer convection.

When the dense layer is thicker, the magma production rate is higher than that of thin dense layer. This may be due to the fact that the dense layer is actively convecting when it is thick. The dense layer is not convecting when it is thin, and the shear coupling between the two layers drags the lower layer flow.

Effects of radioactivity concentration in the dense layer. Although the existence and thickness of the dense layer have limited effect on the core heat flux if the temperature at layer interface is fixed, the radioactivity concentration in the dense layer suppresses core and surface heat fluxes (Figure 2). This is understandable in that a radioactivity concentration in the lower layer increases the lower layer temperature and decreases the core heat flux. Even so, the concentration of radioactivity heating in the dense layer has limited effect on the magma production rate given the new temperature scaling (Figure 3). The slightly decrease of magma production rate may be due to the thickened lithosphere when the surface heat flux is lower.

The absence of a present-day magnetic dynamo places an upper bound on the heat flux out of the core of Mars [24]. Models with realistic rheology can produce plume volcanism while staying below this upper bound [5], but a chemically dense lower mantle layer with radioactivity elements concentration may also contribute to suppressing the core heat flux and the magnetic dynamo, while keeping the magma production roughly unchanged.

Effects of lower viscosity. The shear-coupling between the two layers causes lower magma production rate when the lower layer is thin. By decreasing the lower layer viscosity, the dense layer moves towards independent convection, and the magma production rate becomes higher.

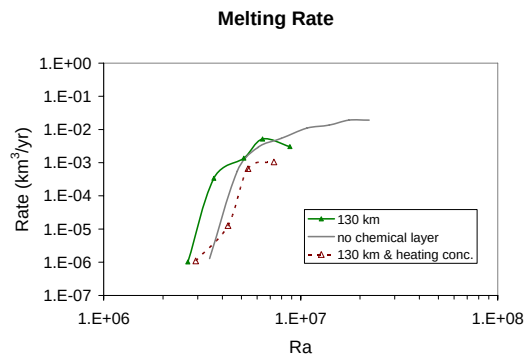

Figure 3. Magma production rate vs upper layer Ra for models with different dense layer thickness and radioactivity elements concentration in the dense layer.

References:[1] Neukum et al., Nature 432, 971-979, 2004. [2] McEwen et al., Icarus 176, 351-381, 2005. [3] Nyquist et al., Space Sci. Rev. 96, 105-164, 2001. [4] Borg et al., Geochim. Cosmochim. Acta 69, 5819-5830, 2005. [5] Li and Kiefer, Geophys. Res. Lett. 34, doi:10.1029/2007GL030544, 2007. [6] Kiefer, Meteoritics Planet. Sci. 38, 1815-1832, 2003. [7] Li and Kiefer, Workshop on Water in Planetary Basalts, Abstract 2011, 2007. [8] Elkins-Tanton et al., Meteoritics Planet. Sci. 38, 1753-1771, 2003. [9] Elkins-Tanton et al., J. Geophys. Res. 110, doi:10.1029/2005JE002480, 2005. [10] Elkins-Tanton et al., Earth Planet. Sci. Lett. 236, 1-12, 2005. [11] Zaranek and Manga, Lunar Planet. Sci. Conf. 38, Abstract 2133, 2007. [12] Li and Kiefer, Lunar Planet. Sci. Conf. 39, Abstract 2023, 2008. [13] Roberts and Zhong, J. Geophys. Res. 109, doi:10.1029/2003JE002226, 2004. [14] Zhong, J. Geophys. Res. 111, doi:10.1029/2005JB003972, 2006. [15] Tackley and King, Geochem. Geophys. Geosyst. 4, 8302, doi:10.1029/2001GC000214, 2003. [16] Mei and Kohlstedt, J. Geophys. Res. 105, 21471-21481, 2000. [17] Wänke and Dreibus, Phil. Trans. R. Soc. London A 349, 285-293, 1994. [18] Montague and Kellogg, J. Geophys. Res. 105, 11101-11114, 2000. [19] Katz et al., Geochem. Geophys. Geosyst. 4, 1073, doi:10.1029/2002GC000433, 2003. [20] Kiefer et al., Workshop on Water in Planetary Basalts, Abstract 2016, 2007. [21] Namiki and Kurita, Geophys. Res. Lett. 30, 1023, doi:10.1029/2002GL015809, 2003. [22] Senshu et al., J. Geophys. Res. 107, 5118, doi:10.1029/2001JE001819, 2002. [23] Righter, Workshop on Early Planetary Differentiation, Abstract 4041, 2006. [24] Nimmo and Stevenson, J. Geophys. Res. 105, 11969-11979, 2000.